



Preparation and characterization of chondroitin-sulfate-A-coated magnetite nanoparticles for biomedical applications



Ildikó Y. Tóth*, Erzsébet Illés, Márta Szekeres, Etelka Tombác*^{*}

Department of Physical Chemistry and Materials Science, University of Szeged, Aradi Vt. 1, H-6720 Szeged, Hungary

ARTICLE INFO

Article history:

Received 17 July 2014

Received in revised form

10 September 2014

Accepted 19 September 2014

Available online 5 November 2014

Keywords:

Superparamagnetic iron oxide nanoparticle (SPION)

Magnetic fluid (MF)

Magnetite

Chondroitin-sulfate

Core-shell nanoparticles

Colloidal stability

Surface charge

ABSTRACT

Polysaccharides are promising candidates for manufacturing biocompatible core-shell nanoparticles with potential *in vivo* use. Superparamagnetic magnetite nanoparticles (MNPs) have prospective application in both diagnosis and therapy, and so developing a novel polysaccharide shell on MNP core is of great challenge. MNPs were prepared by co-precipitation, then the surface of purified MNPs was coated with chondroitin-sulfate-A (CSA) to obtain core-shell structured magnetite nanoparticles (CSA@MNP). The effect of the added amount of CSA on the surface charging and the aggregation state of MNPs at various pHs and 10 mM NaCl was measured by electrophoresis and dynamic light scattering. The amphoteric behavior of MNPs was fundamentally modified by adsorption of CSA polyanions. A very low CSA-loading induces the aggregation of MNPs, while four times more stabilizes the dispersions over the whole pH-range studied. The coagulation kinetics experiments measured at $\text{pH}=6.3 \pm 0.3$ showed that salt tolerance of CSA@MNPs rises up to ~ 150 mM NaCl.

© 2014 Elsevier B.V. All rights reserved.

1. Introduction

Superparamagnetic iron oxide (magnetite, Fe_3O_4 and maghemite, $\gamma\text{-Fe}_2\text{O}_3$) nanoparticles (SPIONs) are in the focus of scientific interest because of their potential biomedical applications such as MRI contrasting, targeted drug delivery and magnetic hyperthermia [1–6]. Most of these applications require the SPIONs to be non-toxic, chemically stable, sufficiently uniform in size, and well-dispersed in aqueous media. The colloidal stability of water-based magnetic fluids (MFs) prepared from SPIONs is of crucial importance under physiological conditions (e.g. in blood $\text{pH} \sim 7.2\text{--}7.4$ and salt concentration ~ 150 mM) because particle aggregation in blood vessels can be disastrous [1–7]. The SPIONs must be coated to prevent aggregation and dissolution of magnetite nanoparticles (MNPs) under physiological conditions [3]. Different organic compounds have been used to coat SPIONs, such as neutral polymers (e.g. natural dextran [8–11]) and polyelectrolytes (e.g. synthetic polyacrylic acid [8,12–14]). Innumerable SPION preparations have been synthesized for biomedical applications,

but only a few of them were characterized systematically in respect of pH-dependent surface charging and aggregation state of coated nanoparticles. Moreover, their salt tolerance would be also important regarding the salty medium and different pH values in the human body.

Dextran- and modified dextran-coated iron oxide nanoparticles are very common magnetic products for biocompatible applications (e.g., Ferumoxides (Feridex or Endorem), Ferumoxtran-10 (Sinerem or Combidex), Ferucarbotran (Resovist) [14,15]). Other polysaccharides are frequently used as coating agents [16], too. One example is chondroitin-sulfate (CS), patented under US 5427767 A [17] and EP-1-433-482-B1 [18]. Chondroitin-sulfate is a natural polysaccharide, which contains a repeating unit of one glucuronic acid and one N-acetyl-galactoseamine, modified by sulfate groups replacing $-\text{OH}$ groups. Depending on the positions and the quantities of the sulfate groups several types of CS can be distinguished, such as chondroitin-sulfate-A (CSA, chondroitin-4-sulfate) and chondroitin-sulfate-C (CSC, chondroitin-6-sulfate) [19] (see Fig. 1). The procedure of magnetic nanoparticle preparation in the presence of CS for potential MRI contrast agents has been patented [17]. Magnetic microspheres with CS-content are offered to use for magnetic targeting [20]. Furthermore, there is a potential for drug delivery, since some promising anticancer drugs, such as multivalent pseudopeptide, bind to chondroitin-sulfate with high affinity [21]. Based on all these, well-defined chondroitin-sulfate-coated core-shell magnetite nanoparticles can be promising candidate for theranostic application.

* Corresponding authors.

E-mail addresses: ildiko.Toth@chem.u-szeged.hu (I.Y. Tóth), tombacz@chem.u-szeged.hu (E. Tombác*).

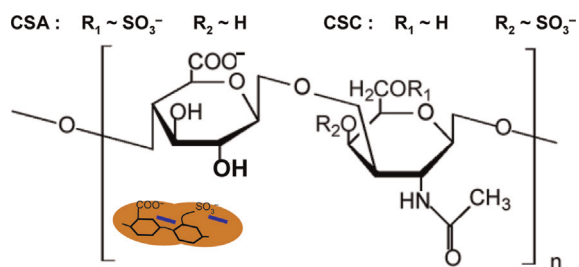


Fig. 1. The repeating unit of fully deprotonated CSA and CSC.

The fundamental aim of our research is the preparation of novel chondroitin-sulfate-coated core-shell magnetite nanoparticles (CSA@MNP) by post-coating method, which are presumably stable colloiddally under physiological condition. We intend to synthesize magnetite nanoparticles by co-precipitation method and to coat them after their purification and characterization. We plan to describe the adsorption of CSA on magnetite and to study the pH-dependent surface charging and aggregation of the CSA@MNP particles. Finally we intend to test the feasibility of the prepared CSA@MNPs in biorelevant media by coagulation kinetics studies.

2. Experimental section

2.1. Materials

The FeCl_2 , FeCl_3 salts and NaOH for magnetite synthesis by co-precipitation [22–26] were analytical grade reagents obtained from Molar, Hungary. The prepared material was purified carefully through washing and dialysis, and it was stored as stable sol at $\text{pH} \sim 3$ and 4°C .

The chondroitin-sulfate-A (CSA) was purchased from Sigma-Aldrich as sodium-salt (Na_2CSA), which could contain a small amount of chondroitin-sulfate-C (CSC), too. One repeating unit of CSA (Fig. 1) contains one $-\text{COOH}$ and one $-\text{SO}_3\text{H}$ group. The strongly acidic sulfate groups ($-\text{SO}_3^-$) in CSA are fully deprotonated at a wide pH-range [27,28]. However, the $-\text{COOH}$ groups in CSA have a pH-dependent dissociation ($\text{pK}_{\beta\text{-glucuronic acid}} \sim 2.9$) [29] given by Eq. (1).



The notation “CSA” is used in this article for sodium-salt regardless of the actual degree of dissociation of the carboxylic groups $\alpha = [-\text{COO}^-]/([-\text{COO}^-] + [-\text{COOH}])$. The amount of CSA is expressed through the mole of repeating units, which equals to the number of dissociable $-\text{COOH}$ groups.

NaCl , HCl and NaOH , analytical grade products of Molar (Hungary) were used to adjust the pH and salt concentration in all experiments. Ultra pure water from a Milli-Q RG water purification system (Millipore) was used. All measurements were performed at $25 \pm 1^\circ\text{C}$.

2.2. X-ray diffraction (XRD)

A Bruker D8 Advance X-ray diffractometer operating in the reflection mode with $\text{Cu-K}\alpha$ radiation was used to take the XRD patterns of synthesized iron oxides. The scanning range of 2θ was between 20° and 80° . The samples of magnetite sol were dried on a glass holder before the measurements. The identification of

magnetite was based on the characteristic peaks in the diffractograms using JCPDS database. The Scherrer equation (see Eq. (2)) was used to calculate the primary particle size:

$$d = (K\lambda)/(B \cos \theta) \quad (2)$$

where d is the average particle size, K is the Scherrer constant (its value is 0.9 for magnetite), λ is the X-ray wavelength (0.154 nm), B is the peak broadening and θ is the position of the peak maximum.

2.3. Magnetic measurement

A vibrating sample magnetometer VSM 880 (DMS/ADE Technologies-USA) was used to measure the magnetization curves at the NCESCF-UP Timisoara. The analysis was performed at room temperature on stable aqueous MNP sol at $\sim 10\%$ by weight; the maximum of the applied field was ~ 840 kA/m. The value of specific magnetization was related to the actual amount of MNP.

2.4. Transmission electron microscopy (TEM)

A Philips CM-10 transmission electron microscope supplied with a Megaview-II camera was used to take the TEM micrographs of iron oxide nanoparticles. The accelerating voltage of 100 kV was applied; the maximum resolution of the instrument is 0.2 nm. One drop of highly diluted magnetite sol was dried on to Formvar-coated copper under infrared lamp. The average size distribution was determined by evaluating 100 particles using the JMicroVision 1.2.7 software.

2.5. Surface modification of MNPs

The surface of the purified, bare magnetite was modified by chondroitin-sulfate-A to prepare core-shell nanoparticles. The effect of the CSA-adsorption on the particle interaction was determined first in concentrated systems at $\text{pH} = 6.3 \pm 0.3$ and 10 mM NaCl . The MNPs were equilibrated for 24 h with CSA solutions of concentration between 0 and 10 mM at a solid/liquid ratio of 20 g/L. The pH was adjusted at the beginning of adsorption. The adsorption series was evaluated after a day.

2.6. Particle size determination

For characterization of the aggregation state of nanoparticles, the average hydrodynamic diameter ($Z\text{-Ave}$) of bare magnetite particles and of CSA-coated nanoparticles were determined at $25 \pm 0.1^\circ\text{C}$ using dynamic light scattering (DLS) method, an apparatus Nano ZS (Malvern) with a 4 mW He-Ne laser source ($\lambda = 633$ nm) operating in backscattering mode at an angle of 173° . The dispersions were diluted to get an optimal intensity of $\sim 10^5$ counts per s, thus the samples contained 100 mg/L of magnetite. Prior to the measurements, the samples were homogenized in an ultrasonic bath for 10 s, after which 2 min relaxation was allowed. Any changes in the aggregation state of the bare or the CSA-coated nanoparticles in aqueous dispersions was characterized by the hydrodynamic diameter ($Z\text{-Ave}$). The influence of the added CSA amount was determined at $\text{pH} = 6.3 \pm 0.3$ and 10 mM NaCl . The effect of pH variation (between 3 and 10) at different CSA-loadings (0.0, 0.05, 0.1, 0.2, and 0.4 mmol/g) was studied at 10 mM NaCl . For evaluation, we used the second- or third-order cumulant fit of the autocorrelation functions, depending on the degree of polydispersity.

2.7. Electrokinetic potential measurements

Electrophoretic mobilities of the pure magnetite and CSA@MNP dispersions were measured at 25 ± 0.1 °C in the same Nano ZS (Malvern) apparatus using disposable zeta cells (DTS 1060). The zeta-standard of Malvern (-55 ± 5 mV) was used for calibration. The added amounts of CSA, the pH-range, and the ionic strength were identical to those in the DLS experiments. The Smoluchowski equation was applied to convert electrophoretic mobilities to electrokinetic potential values. The accuracy of the measurements was ± 5 mV.

2.8. Salt tolerance tests

The CSA-adsorption can change the colloidal stability of the magnetite nanoparticles and this process can be tested accurately in coagulation kinetics experiments. These measurements were performed at different NaCl concentrations, 25 ± 0.1 °C, pH = 6.3 ± 0.3 and 0.2 mmol/g CSA-loading. The change in the hydrodynamic diameter of kinetic units (Z-Ave) was measured by DLS for 15 min; the resolution was 1 min. At a given NaCl concentration, the measured Z-Ave data were plotted as a function of time. The initial slope of the curve is proportional to the coagulation rate [30,31] and the ratio of the fast and slow coagulation rates results in the stability ratio (W). The critical coagulation concentration (CCC) was determined from the stability plot (the dependence of the stability ratio on the NaCl concentration, $\log_{10} W = f(\log_{10} c)$ [22,23]) as the intersection point of straight lines fitted to the experimental $\log_{10} W$ values belonging to the slow and fast coagulation regimes.

The majority of the experiments were performed at pH = 6.3 ± 0.3 and 10 mM NaCl. For the sake of simplicity, we take this pH value as pH ~ 6.3 and omit the indication of pH and NaCl concentration unless it has special significance or the values are different.

3. Results and discussion

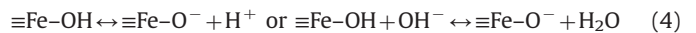
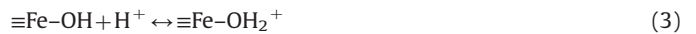
3.1. Characterization of the prepared magnetite nanoparticles

XRD, TEM and VSM methods were used to characterize the crystalline phase, the primary particle size and the magnetic property of the prepared iron oxide particles. The results can be seen in Fig. 2a–c.

The X-ray diffractogram (Fig. 2a) shows the crystalline structure of the synthesis product. The typical peaks can be found at 30.1° , 35.5° , 43.2° , 57.0° and 63.0° , which preferably correspond to the magnetite according to the JCPDS database. The Miller indices of these peaks are (220), (311), (400), (511) and (440), respectively. The primary particle size calculated from the peak at 35.5° with Scherrer equation was about 10 nm. The TEM picture (Fig. 2c) of the MNPs shows spherical particles and their calculable average size was around 10 nm, too. The magnetization curve of the naked MNP (Fig. 2b) shows no hysteresis, and so the magnetic behavior of the synthesized nanoparticles is superparamagnetic at room temperature. This property is in a good agreement with the primary particle size, because the superparamagnetic limit of magnetite nanoparticles is ~ 20 nm [32,33]. The value of the saturation magnetization is ~ 75 emu/g.

The pH-dependent surface charging and aggregation of naked magnetite were determined by electrokinetic potential and dynamic light scattering measurements (Fig. 2d). To understand the significant changes shown in Fig. 2d, first the surface charging of naked MNPs needs to be clarified in general. The surface of magnetite becomes charged, when particles are dispersed in aqueous

media [22,23,32,34–40]. Charges develop on the amphoteric surface hydroxyls ($\equiv\text{Fe}-\text{OH}$) and this process is controlled by both the pH and the ionic strength of aqueous medium [22,23,41–44]. The reactions of surface $\equiv\text{Fe}-\text{OH}$ sites with H^+ and OH^- ions lead to the formation of positive ($\equiv\text{Fe}-\text{OH}_2^+$) and negative ($\equiv\text{Fe}-\text{O}^-$) surface charges (see Eqs. (3) and (4)).



At a characteristic pH, i.e., the pH of isoelectric point (IEP), the amounts of oppositely charged surface sites are equal to each other. At pHs lower than the IEP, the charge of MNP is positive due to the presence of excess $\equiv\text{Fe}-\text{OH}_2^+$ groups, while the particles are negatively charged above the pH of IEP because of the formation of $\equiv\text{Fe}-\text{O}^-$ groups, the IEP of magnetite is often in wide pH-range [32].

As shown on the inserted photos of Fig. 2d, colloidal stable dispersion of naked magnetite can only be observed at pH values below 5 or above 10, accompanied by a high absolute value of electrokinetic potential (+40 mV or –40 mV) and a low hydrodynamic diameter (~ 120 nm), because of the electrostatic stabilization of particles, caused by the presence of either $\equiv\text{Fe}-\text{OH}_2^+$ in the acid range or $\equiv\text{Fe}-\text{O}^-$ surface groups in the basic range. The measured IEP of magnetite nanoparticles, where the electrokinetic potential of MNPs is zero is at pH ~ 8. Around this pH, close to the physiological conditions (e.g. in blood pH 7.2–7.4), the naked MNPs are aggregated (the average particle size ~ 1600 nm). In biological milieu like blood, this would be dangerous because of embolism. So the pH-range of aggregation must be shifted in order to have a chance for biomedical applications. Therefore the surface of MNPs should be modified to overcome this gap, here we use CSA to coat MNPs.

3.2. CSA-loading of magnetite nanoparticles

The series of magnetite sols loaded with CSA at pH ~ 6.3 after standing for 24 h is presented in Fig. 3. With increasing CSA concentration, the colloidal state of samples changes characteristically from aggregated to stable. In these samples, the solution concentration of CSA increases from 0 to 9 mmol/L (expressed through the molar amount of its repeating units), while its specific amount related to 1 g magnetite rises up to 0.45 mmol/g.

To understand this significant change shown in Fig. 3, we have to evaluate the surface charging of naked magnetite at the given condition, i.e., at the pH ~ 6.3 and 10 mM NaCl. Under these conditions the amount of the positive charge on MNPs is ~ 0.05 mmol/g from acid/base titration [12]. This is not enough to stabilize the particles electrostatically; therefore, the naked MNPs are aggregated and settled (see the first vial in Fig. 3). With increasing CSA-loading, firstly the CSA@MNP particles are still settled, but above ~ 0.25 mmol/g CSA addition, the CSA-coated magnetite nanoparticles become dispersed (see the sixth vial in Fig. 3). The CSA@MNP samples seem to be stable at high CSA-loading (see the last three photos in Fig. 3), but the signs of aggregation (particles on the glass surface and partial sedimentation) can be seen even under these conditions. However, stable magnetic fluid can be prepared from the CSA-coated MNPs by careful addition of CSA to magnetite sol under vigorous mixing.

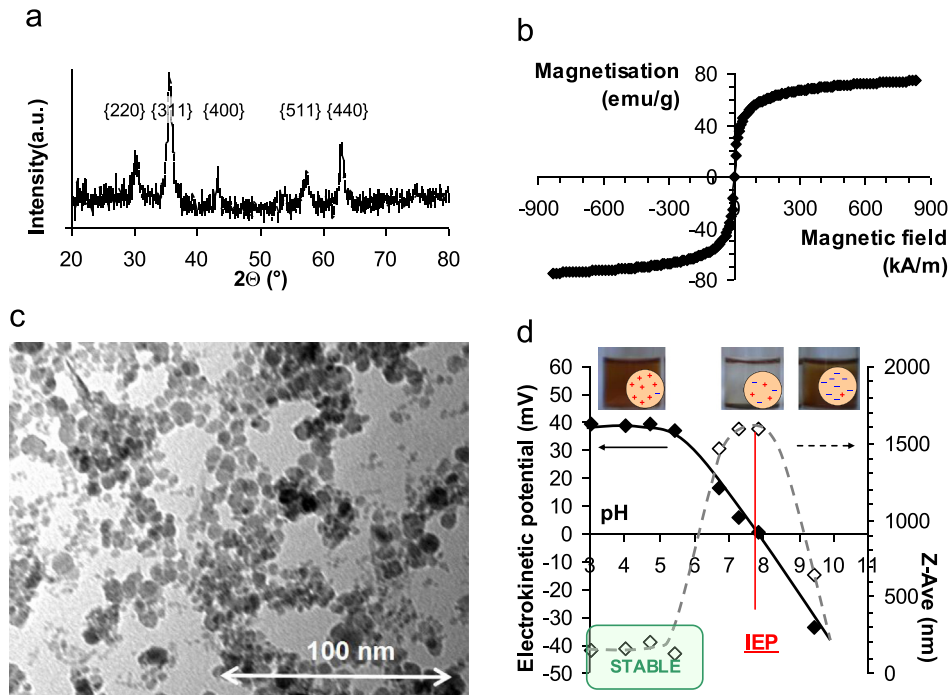


Fig. 2. Characterization of the naked magnetite nanoparticles by (a) XRD pattern, (b) specific magnetization curve, (c) TEM image and by (d) the pH-dependent electrokinetic potential and average size (Z-Ave) measured at 10 mM NaCl by DLS. (Photos were taken after standing for 24 h, the inserted pictures are the schematic illustration of the surface charging on MNPs. Lines are drawn as guides for the eye.)

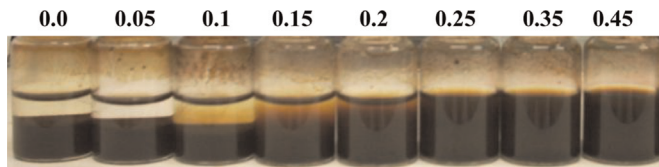


Fig. 3. Series of CSA adsorption on MNP, containing CSA in increasing amount up to 0.45 mmol/g (see the numbers on the vials) at pH~6.3 and 10 mM NaCl at a solid/liquid ratio of 20 g/L. (The amount of CSA is expressed through the molar amount of repeating units given in mmol, normalized to 1 g magnetite).

3.3. Surface charging and colloidal stability of CSA-coated core-shell MNPs

The changes in the electrokinetic potential and the average size (Z-Ave) of the nanoparticles are plotted as a function of CSA addition in Fig. 4a. A few representative samples are shown in Fig. 4b along with a schematic illustration of the CSA-coating of particles. As discussed earlier, the naked magnetite is positively charged at pH~6.3 and 10 mM NaCl, the electrokinetic potential of the particles is $\sim +25$ mV, and the sample is aggregated (Z-Ave ~ 1500 nm) and settled (see the first vial in Fig. 4b). The electrokinetic potential declines with the increasing amount of negatively charged CSA due to the $-\text{SO}_3^-$ and $-\text{COO}^-$ groups, added gradually to the MNP sols. The charge neutralization levels at ~ 0.035 mmol/g CSA-loading. This is a kind of isoelectric point (IEP), where negatively charged CSA patches exist on the positive MNPs and these patchwise charge heterogeneity induces particles aggregation and drives the Z-Ave of CSA@MNP aggregates to a maximum (~ 2300 nm). Further addition of chondroitin-sulfate-A caused charge reversal, decreased the value of the electrokinetic potential to ~ -45 mV, and brought about the electrosteric stabilization of CSA@MNP samples (see in Fig. 4a). The particles become fully dispersed and colloidally stable (Z-Ave ~ 120 nm) at ~ 0.2 mmol/g of CSA addition (see the last vials in Fig. 4b).

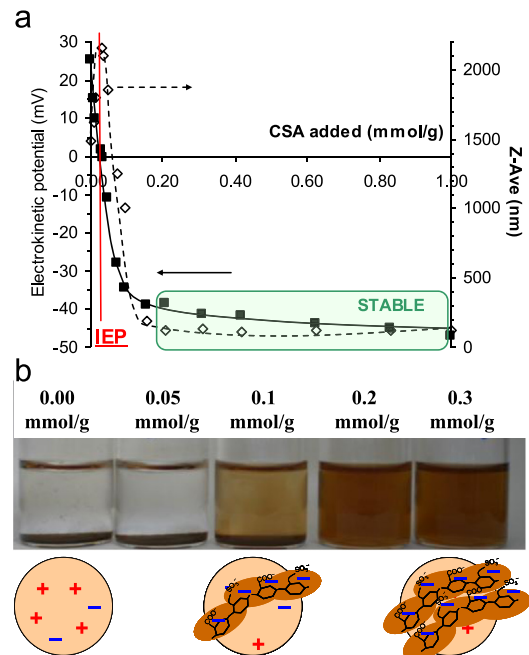


Fig. 4. Effect of CSA addition (a) on the electrokinetic potential and average size (Z-Ave) of MNPs and (b) on the colloidal stability of the dispersions at pH~6.3 and 10 mM NaCl (photos were taken after standing for 24 h) in parallel with the schematic illustration of CSA-coating of particles. (Lines are drawn as guides for the eye. The amount of CSA is expressed through the molar amount of repeating units given in mmol.)

The pH-dependent electrokinetic potential, the average particle size and the photos showing the change in colloidal stability of the CSA@MNP particles at different CSA-loadings (0.0, 0.05, 0.1, 0.2 and 0.4 mmol/g) can be seen in Fig. 5. The pH-dependent properties of naked magnetite were already discussed in Section 3.1. Adding a small amount of CSA (0.05 mmol/g) to the MNP, the

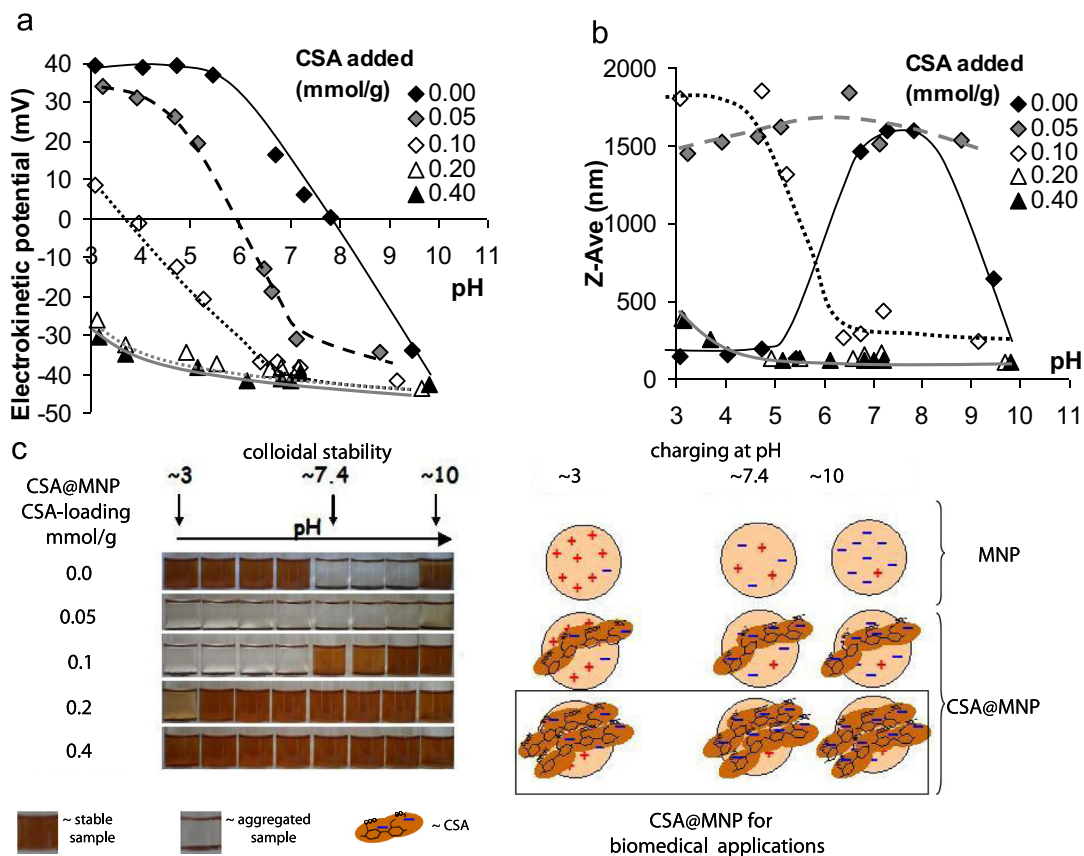


Fig. 5. pH-dependent (a) electrokinetic potential, (b) average particle size and (c) colloidal stability of the dispersions at 10 mM NaCl after standing for 24 h in parallel with the schematic illustration of CSA-coating of particles. The series of MNPs at CSA-loadings 0.0, 0.05, 0.1, 0.2 and 0.4 mmol/g are presented. (Lines are drawn as guides for the eye. Pictures were taken a day after the pH setting between 3 and 10.)

IEP decreases from pH ~8 to pH ~6 and the particles aggregate over the whole range of pH studied here, due to the patchwise adsorption of the negatively charged CSA on the originally positively charged MNP [22,23,45,46]. Increasing amounts of CSA shift the IEP gradually to a more acidic pH value (Fig. 5a) and narrow the pH-range of aggregation (Fig. 5b and c). Further addition of CSA (above ~0.2 mmol/g) results in stable MNP dispersion with low particle size and electrokinetic potential almost over the whole pH-range studied.

3.4. Salt tolerance of CSA-coated core-shell MNPs

The salt tolerance of MNPs coated with 0.2 mmol CSA/g was studied in coagulation kinetics experiments at pH~6.3. The particle size evolution was followed in time by DLS experiments (see Fig. 6a) and the calculated stability ratios ($\log_{10} W$) are plotted as a function of NaCl concentration ($\log_{10} c$) in Fig. 6b. The critical coagulation concentration (CCC) was determined (see Fig. 6b) to characterize accurately the salt tolerance of the CSA@MNP

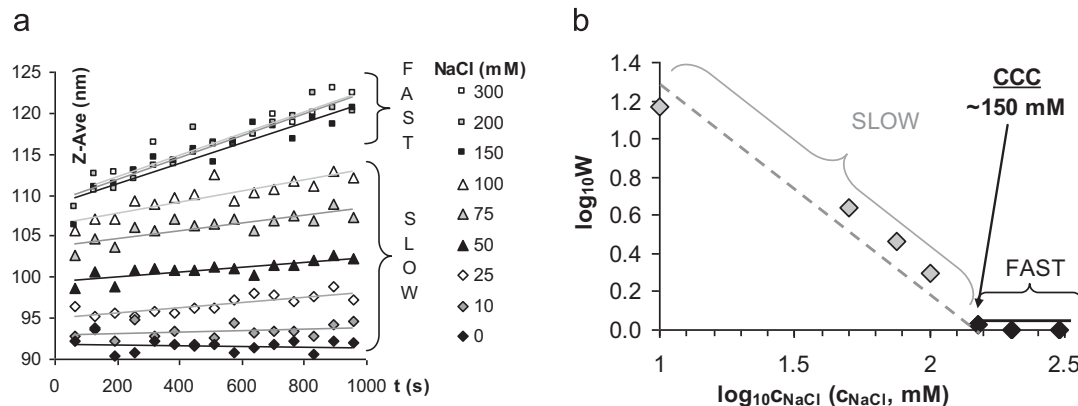


Fig. 6. Coagulation kinetics measured by dynamic light scattering: (a) time-dependent increase in average size and (b) stability plot indicating the slow and fast coagulation regimes to determine the CCC value of the CSA@MNP sample (0.2 mmol CSA/g magnetite) at pH~6.3. (Lines are drawn as guides for the eye.)

dispersion. The CCC of naked MNP is ~ 1 mM NaCl at $\text{pH} \sim 6.3$ [12,47], however, the CCC of CSA@MNP at 0.2 mmol/g CSA-loading is much higher ~ 150 mM owing to the effective polyanionic coverage of MNP's surface. This CCC value is high enough to enable the use of CSA@MNP at physiological concentration of NaCl.

4. Conclusion

The aim of this work was to prepare novel CSA-coated core-shell magnetite nanoparticles stable colloiddally under physiological condition and to characterize the surface coating process and the surface-properties of the CSA@MNP product as well. The solid experimental facts allow us to conclude that the CSA@MNP particles can be prepared, which are electrosterically stabilized at CSA-loading > 0.2 mmol/g over the wide range of pH (> 4) matching well with biological medium. The measured CCC guarantees that the salt tolerance of CSA@MNP is sufficiently high to resist aggregation in a physiological medium. So the CSA-coated core-shell magnetite nanoparticles are promising candidates for biomedical applications like contrast agents in MRI diagnostics or well defined carriers in drug delivery for anticancer drugs. Furthermore, based on the potential combination of these medical diagnostic and therapeutic methods, even the theranostic application of CSA@MNP products can be feasible.

Acknowledgment

This work was supported by OTKA (NK 84014) foundation. The authors are grateful to Dr. Vlad Socoliuc (Center of Fundamental and Advanced Technical Research of the Timisoara Branch of Romanian Academy) for the magnetic measurements.

References

- [1] E. Amstad, M. Textora, E. Reimhult, Stabilization and functionalization of iron oxide nanoparticles for biomedical applications, *Nanoscale* 3 (2011) 2819–2843.
- [2] N. Fauconnier, A. Bée, J. Roger, J.N. Pons, Synthesis of aqueous magnetic liquids by surface complexation of maghemite nanoparticles, *J. Mol. Liq.* 83 (1999) 233–242.
- [3] Q.A. Pankhurst, J. Connolly, S.K. Jones, J. Dobson, Applications of magnetic nanoparticles in biomedicine, *J. Phys. D: Appl. Phys.* 36 (2003) R167–R181.
- [4] A.K. Gupta, M. Gupta, Synthesis and surface engineering of iron oxide nanoparticles for biomedical applications, *Biomaterials* 26 (2005) 3995–4021.
- [5] T.K. Jain, J. Richey, M. Strand, D.L. Leslie-Pelecky, C.A. Flask, V. Labhasetwar, Magnetic nanoparticles with dual functional properties: drug delivery and magnetic resonance imaging, *Biomaterials* 29 (2008) 4012–4021.
- [6] E. Munnier, S. Cohen-Jonathan, C. Linassier, L. Douziech-Eyrolles, H. Marchais, M. Soucé, K. Hervé, P. Dubois, I. Chourpa, Novel method of doxorubicin-SPION reversible association for magnetic drug targeting, *International Journal of Pharmaceutics*. Int. J. Pharm. 363 (2008) 170–176.
- [7] C. Boyer, M.R. Whittaker, V. Bulmus, J. Liu, T.P. Davis, The design and utility of polymer-stabilized iron-oxide nanoparticles for nanomedicine applications, *NPG Asia Mater.* 2 (2010) 23–30.
- [8] S. Laurent, D. Forge, M. Port, A. Roch, C. Robic, L. Vander-Elst, R.N. Muller, Magnetic iron oxide nanoparticles: synthesis, stabilization, vectorization, physicochemical characterizations, and biological applications, *Chem. Rev.* 108 (2008) 2064–2110.
- [9] M. Hasegawa, S. Hokkoku (1978), Magnetic iron oxide-dextran complex and process for its production, United States Patent 4101435.
- [10] D. Kirpotin; D.C.F. Chan, P.A. Bunn, Jr. (1995), Magnetic microparticles, United States Patent 5411730.
- [11] M. Mahdavi, M.B. Ahmad, M.J. Haron, F. Namvar, B. Nadi, M.Z.A. Rahman, J. Amin, Synthesis, surface modification and characterisation of biocompatible magnetic iron oxide nanoparticles for biomedical applications, *Molecules* 18 (2013) 7533–7548.
- [12] A. Hajdú, M. Szekeres, I.Y. Tóth, R.A. Bauer, J. Mihály, I. Zupkó, E. Tombácz, Enhanced stability of polyacrylate-coated magnetite nanoparticles in bio-relevant media, *Colloids Surf. B: Biointerfaces* 94 (2012) 242–249.
- [13] A. Jedlovszky-Hajdú, E. Tombácz, I. Bányai, M. Babos, A. Palkó, Carboxylated magnetic nanoparticles as MRI contrast agents: relaxation measurements at different field strengths, *J. Magn. Magn. Mater.* 324 (2012) 3173–3180.
- [14] M. Szekeres, I.Y. Tóth, E. Illés, A. Hajdú, I. Zupkó, K. Farkas, G. Oszlanczi, L. Tiszlavicz, E. Tombácz, Chemical and colloidal stability of carboxylated core-shell magnetite nanoparticles designed for biomedical applications, *Int. J. Mol. Sci.* 14 (2013) 14550–14574.
- [15] Y.W. Jun, J.H. Lee, J. Cheon, Nanoparticle contrast agents for molecular magnetic resonance imaging, in: C.A. Mirkin, C.M. Niemeyer (Eds.), *Nanobiotechnology II: More Concepts and Applications*, Wiley, Weinheim, 2007.
- [16] C. Lemarchanda, R. Grefa, P. Couvreur, Polysaccharide-decorated nanoparticles, *Eur. J. Pharm. Biopharm.* 58 (2004) 327–341.
- [17] M. Kresse, R. Lawaczek, D. Pfeifferer (1995), Nanocrystalline magnetic iron oxide particles-method for preparation and use in medical diagnostics and therapy, United States Patent 5427767.
- [18] S. Nishida, N. Katayama, T. Katsumata, M. Sato (2006), Aqueous preparation containing a shark-derived chondroitin iron sulfate colloid, European Patent 1433482 B1.
- [19] R.M. Lauder, Chondroitin sulphate: a complex molecule with potential impacts on a wide range of biological systems, *Complement. Ther. Med.* 17 (2009) 56–62.
- [20] D.B. Kirpotin, R. Kinne, A. Milton, E. Palombo-Kinnic, F. Emmrich, Magnetic targeting of a therapeutic antibody using magnetotropic microspheres of the interpolyelectrolyte coacervation complex, *J. Magn. Magn. Mater.* 122 (1993) 354–359.
- [21] D. Destouches, N. Page, Y. Hamma-Kourbali, V. Machi, O. Chaloin, S. Frechault, C. Birmpas, P. Katsoris, J. Beyrath, P. Albanese, M. Maurer, G. Carpentier, J.-M. Strub, A. Van Dorsselaer, S. Muller, D. Bagnard, J.P. Briand, J. Courty, A simple approach to cancer therapy afforded by multivalent pseudopeptides that target cell-surface nucleoproteins, *Cancer Res.* 71 (2011) 3296–3305.
- [22] E. Illés, E. Tombácz, The role of variable surface charge and surface complexation in the adsorption of humic acid on magnetite, *Colloids Surf. A: Physicochem. Eng. Asp.* 230 (2006) 99–109.
- [23] E. Illés, E. Tombácz, The effect of humic acid adsorption on pH-dependent surface charging and aggregation of magnetite nanoparticles, *J. Colloid Interface Sci.* 295 (2006) 115–123.
- [24] L. Vékás, D. Bica, O. Marinica, Magnetic nanofluids stabilized with various chain length surfactants, *Rom. Rep. Phys.* 58 (2006) 217–228.
- [25] D. Bica, L. Vékás, M.V. Avdeev, O. Marinica, V. Socoliuc, M. Balasoiu, V. M. Garamus, Sterically stabilized water based magnetic fluids: synthesis, structure and properties, *J. Magn. Magn. Mater.* 311 (2007) 17–21.
- [26] E. Tombácz, E. Illés, A. Majzik, A. Hajdú, N. Rideg, M. Szekeres, Ageing in the inorganic nanoworld: example of magnetite nanoparticles in aqueous medium, *Croat. Chem. Acta* 80 (2007) 503–515.
- [27] M. Bathe, G.C. Rutledge, A.J. Grodzinsky, B. Tidor, A. Coarse-Grained, Molecular model for glycosaminoglycans: application to chondroitin, chondroitin sulfate, and hyaluronic acid, *Biophys. J.* 88 (2005) 3870–3887.
- [28] R.L. Cleland, Electrophoretic mobility of wormlike chains. I. Experiment: hyaluronate and chondroitin 4-sulfate, *Macromolecules*, 24, 4386–4390.
- [29] H. Wang, D. Loganathan, R.J. Linhardt, Determination of the pKa of glucuronic acid and the carboxy groups of heparin by 13 C-nuclear-magnetic-resonance spectroscopy, *Biochem. J.* 278 (1991) 689–695.
- [30] M. Elimelech, J. Gregory, X. Jia, R.A. Williams, *Particle Deposition and Aggregation: Measurement, Modeling and Simulation*, Butterworths, Oxford, 1995.
- [31] D.J. Shaw, *Introduction to Colloid and Surface Chemistry*, Butterworths, London, 1966.
- [32] R.M. Cornell, U. Schwertmann, *The Iron Oxides. Structure, Properties, Reactions, Occurrence and Uses*, VCH, Weinheim, 1996.
- [33] D.J. Dunlop, Ö Özdemir, *Rock Magnetism*, Cambridge University Press, Cambridge, 1997.
- [34] C.T. Johnston, E. Tombácz, Surface chemistry of soil minerals, in: J.B. Dixon, D. G. Schulze (Eds.), *Soil Mineralogy with Environmental Applications*, SSSA, Madison, Wisconsin, 2002.
- [35] G. Sposito, *The Surface Chemistry of Soils*, Oxford University Press, Oxford, 1984.
- [36] T. Hiemstra, W.H. van Riemsdijk, Fluoride adsorption on goethite in relation to different types of surface sites, *J. Colloid Interface Sci.* 225 (2000) 94–104.
- [37] R.P.J.J. Rietra, T. Hiemstra, W.H. van Riemsdijk, Electrolyte anion affinity and its effect on oxyanion adsorption on goethite, *J. Colloid Interface Sci.* 229 (2000) 199–206.
- [38] L.G.J. Fokkink, A. de Keizer, J. Lyklema, Specific ion adsorption on oxides: Surface charge adjustment and proton stoichiometry, *J. Colloid Interface Sci.* 118 (1987) 454–462.
- [39] G. Sposito, Characterization of particle surface charge, in: J. Buffle, H.P. van Leeuwen (Eds.), *Environmental Particles*, Lewis, Boca Raton, 1992.
- [40] Z.X. Sun, F.W. Su, W. Forsling, P.O. Samskog, Surface characteristics of magnetite in aqueous suspension, *J. Colloid Interface Sci.* 197 (1998) 151–159.
- [41] J. Lyklema, Structure of the solid/liquid interface and the electrical double layer, in: ThF. Tadros (Ed.), *Solid/Liquid Dispersions*, Academic Press, London, 1987.
- [42] J. Lyklema, Nomenclature, symbols, definitions and measurements for electrified interfaces in aqueous dispersions of solids, *Pure Appl. Chem.* 63 (1991) 895–906.
- [43] J. Lyklema, *Fundamentals of Interface and Colloid Science*, Academic Press, London, 1995.

- [44] R.O. James, G.A. Parks, Characterization of aqueous colloids by their electrical double-layer and intrinsic surface chemical properties, in: E. Matijevic (Ed.), *Surface and Colloid Science*, Plenum Press, New York, 1982.
- [45] J. Gregory, Flocculation by polymers and polyelectrolytes, in: ThF. Tadros (Ed.), *Solid/Liquid Dispersions*, Academic Press, London, 1987.
- [46] M. Borkovec, G. Papastavrou, Interactions between solid surfaces with adsorbed polyelectrolytes of opposite charge, *Curr. Opin. Colloid Interface Sci.* 13 (2008) 429–437.
- [47] I.Y. Tóth, E. Illés, R.A. Bauer, D. Nesztor, M. Szekeres, I. Zupkó, E. Tombácz, Designed polyelectrolyte shell on magnetite nanocore for dilution-resistant biocompatible magnetic fluids, *Langmuir* 28 (2012) 16638–16646.